120
1/4/93 (2)

NIPER-629
(DE93000105)

Modeling and Laboratory Investigations of Microbial Oil Recovery Mechanisms in Porous Media

Topical Report

By
Ming-Ming Chang
Rebecca S. Bryant
Anita K. Stepp
Kathy M. Bertus

December 1992

Performed Under Cooperative Agreement No. FC22-83FE60149

IIT Research Institute
National Institute for Petroleum and Energy Research
Bartlesville, Oklahoma

Bartlesville Project Office
U. S. DEPARTMENT OF ENERGY
Bartlesville, Oklahoma

NIPER-629
Distribution Category UC-122

Modeling and Laboratory Investigations of Microbial Oil Recovery Mechanisms in Porous Media

Topical Report

NIPER--629

DE93 000105

By
Ming-Ming Chang
Rebecca S. Bryant
Anita K. Stepp
Kathy M. Bertus

December 1992

Work Performed Under Cooperative Agreement No. DE-FC22-83FE60149

Prepared for
U.S. Department of Energy
Assistant Secretary for Fossil Energy

Rhonda Patterson, Project Manager
Bartlesville Project Office
P. O. Box 1398
Bartlesville, OK 74005

Prepared by
IIT Research Institute
National Institute for Petroleum and Energy Research
P.O. Box 2128
Bartlesville, OK 74005

TABLE OF CONTENTS

Page

ABSTRACT 1
INTRODUCTION 1
DESCRIPTION OF MATHEMATICAL MODEL 2
Transport Formulation 3
Oil Recovery Model 4
Numerical Solution 5
EXPERIMENTAL APPARATUS, PROCEDURES, AND RESULTS 5
Coreflood Apparatus and Procedures 6
Crude Oil 6
Microorganisms 6
Chemicals and Media 6
Unsteady-State Relative Permeability Tests 6
CT Imaging 6
Experimental Results 7
Microbial Retention Tests 7
Pressure Profile 7
Unsteady-State Relative Permeability Tests 7
CT Imaging Experiments 8
SIMULATION OF COREFLOOD EXPERIMENTS 8
Diffusion 9
Adsorption 9
Microbial Concentration Profile 9
Pressure Profile 9
FIELD-SCALE SIMULATIONS 10
CONCLUSIONS 11
ACKNOWLEDGEMENTS 11
NOMENCLATURE 12
REFERENCES 13

TABLES

Page

1. Core properties and microbial system parameters used in matching pressure drop in a microbial coreflood 15
2. Summary of unsteady-state relative permeability tests 15
3. Microbial system parameters used in simulations 16
4. Core properties and microbial system parameters used in matching microbial effluent profiles 16
5. Core properties and microbial system parameters used in simulating microbial and nutrient concentration profiles 16
6. Core properties and microbial system parameters used in matching pressure drop in microbial coreflood 17
7. Reservoir model and microbial system parameters used in field-scale simulations 17
8. Reservoir and fluid parameters used in numerical field simulations 18

ILLUSTRATIONS

1. Shift of wettability of siloxane-treated cores after microbial treatments 18
2. Recovery of microorganisms vs. amount injected in coreflood experiments 19
3. Pressure drops during microbial corefloods, and simulation matches 19
4. CT/image of core after microbial treatment showing gas saturation. Scale is in Houndsfield units 20
5. CT/image of core at residual oil saturation after waterflooding and core after microbial treatment and subsequent waterflooding. Scale is in Houndsfield units 21
6. Microbial concentration and sugar consumption in a flask test 22
7. Simulations match of experimental tracer data in a 4-ft long Berea sandstone core 22

8a. Simulation match of the microbial concentration in coreflood effluent after 0.75 PV injection 23

8b. Simulation match of the microbial concentration in coreflood effluent after 1.0 PV injection 23

8c. Simulation match of the microbial concentration in coreflood effluent after 1.5 PV injection 24

ILLUSTRATIONS - Continued

Page

9a. Results of simulation of the microbial concentration profile through a 4-ft long Berea sandstone core after 0.5 PV waterflood 24

9b. Results of simulation of the nutrient concentration profile through a 4-ft long Berea sandstone core after 0.5 PV waterflood 25

10. Simulation match of pressure drop and porosity change in a microbial coreflood.. 25

11. Microbial profiles for reservoirs with various clogging rate constants 26

12. Effect of chemotaxis coefficient k_m on microbial concentration profile..... 26

13. Fractional injection into low permeability layer 27

14. Injection profile modification using microbial treatment 27

15. Field-scale numerical simulation of oil recoveries resulting from changes in relative permeabilities from R1 test and after microbial treatment (R2) 28

MODELING AND LABORATORY INVESTIGATION OF MICROBIAL OIL RECOVERY MECHANISMS IN POROUS MEDIA

By Ming-Ming Chang, Rebecca S. Bryant, Anita K. Stepp, and Kathy M. Bertus

ABSTRACT

Simulation and experimental results on the transport of microbes and nutrients in one-dimensional cores are presented, and the development of a three-dimensional, three-phase, multiple-component numerical model to describe the microbial transport and oil recovery in porous media is described. The change of rock's wettability and associated relative permeability values after microbial treatments were accounted for in the model for additional oil recovery. Porosity and permeability reductions due to cell clogging have been considered and the production of gas by microbial metabolism has been incorporated. Governing equations for microbial and nutrient transport are coupled with continuity and flow equations under conditions appropriate for a black oil reservoir.

From our concepts of the hydrodynamics, physics, chemistry and microbiology of microbial oil recovery (MEOR) processes, microbial parameters incorporated into the microbial transport model include: (1) microbial growth and decay; (2) microbial deposition; (3) chemotaxis; (4) diffusion; (5) convective dispersion; (6) tumbling; and (7) nutrient consumption. Laboratory experiments were conducted to obtain actual data for the simulator regarding microbial growth and decay, nutrient consumption, microbial deposition, convective dispersion, and diffusion. Unsteady-state relative permeability measurements using microbial formulations were made to determine the effects of microbial metabolites on fractional fluid flow in porous media. Mechanisms considered to be important for oil recovery include changes in microscopic properties such as interfacial tension, wettability, and adsorption that govern oil mobilization and affect fractional flow and relative permeability. Other oil recovery mechanisms traditionally associated with fluid flow changes include polymer and biomass production by microorganisms. Computer tomography studies demonstrated that gas production by microorganisms in porous media can reduce residual oil saturation in porous media.

The computer simulator has been used to determine the effects of various transport parameters on microbial transport phenomena. The model can accurately describe the observed transport of microbes, nutrients, and metabolites in coreflooding experiments. Input parameters are determined by matching laboratory experimental results. The model can be used to predict the propagation of microbes and nutrients in a model reservoir and to optimize injection strategies. Optimization of injection strategy results in increased oil recovery due to improvements in sweep efficiency. Field-scale numerical simulation studies using data from relative permeability experiments indicated that microbial treatment could improve oil recovery over waterflooding alone. This report addresses the work conducted under project BE3 of the NIPER FY92 annual plan.[1]

INTRODUCTION

Microbial methods for increasing oil recovery are potentially cost-effective even at relatively low crude oil prices. Microbial formulations can be applied in a variety of methods including permeability modification treatments and microbial-enhanced waterflooding.[2-4] The flexibility and potential cost-effectiveness of the technology make it attractive, but further understanding of the transport mechanisms of microorganisms and the development of a sound engineering methodology for optimizing microbial formulations and injection strategies are needed to realize its potential.

The transport of microorganisms (bacteria, fungi, and viruses) in porous media governs many phenomena in bioremediation of environmental pollution problems and microbial enhanced oil recovery. The purpose of this study is to investigate the oil recovery mechanisms and effects of transport parameters of microbes to modify reservoir heterogeneities and improve oil recovery. The transport of microorganisms in subsurface formations is governed by many complicated physical, chemical, and biological phenomena such as adsorption, interaction between microorganisms and substrate, and growth and decay of cells.[5-9] Information concerning the transport, growth, and metabolism of viable cells in subsurface environments is scarce, and some of the phenomena are still not well understood.

Although several attempts have been made to describe microbial processes,[10-12] no model has yet fully incorporated all of the complex phenomena that are believed to be important. The unusual complexity of oil recovery by microbial formulations requires close coordination between laboratory mechanistic studies and oil displacement experiments under carefully controlled conditions to develop and validate a computer model. The accuracy of a simulator that is designed for MEOR processes will be strongly dependent upon the accuracy of the equations that are used to describe the important phenomena. An accurate reservoir simulator for MEOR methods can best be developed through an integrated program of acquisition of laboratory and field data with the feedback loop being the reservoir simulation model.

In this report, the mathematical formulation of microbial transport and oil recovery model in the porous media was described first. The governing transport equations in the model include net flux of microbes by convection and dispersion, decay and growth rates of microbes, chemotaxis, nutrient consumption, and deposition of microbes on rock grain surfaces. The change of rock's wettability and associated relative permeability values after microbial treatments were accounted for in the model as oil recovery mechanisms. This is followed by discussions of laboratory experiments which were conducted with microbial isolates that produce mainly gases and surfactants when fermenting sugars such as those present in molasses. Unsteady-state relative permeability measurements were conducted using a surfactant-producing microorganism. CT imaging experiments using microorganisms were conducted to evaluate the production of gas inside a Berea sandstone core and determine the effects of trapped gas saturation on improved oil recovery by microbial formulations. Results from microbial coreflooding experiments were used to determine microbial transport parameters for the simulator. Laboratory data were used to develop correlations and mathematical models for specific phenomena; linear coreflooding data were used to test the simulator in an iterative process. Finally, field-scale simulations of microbial treatments were conducted to study the oil recovery and microbial transport in reservoirs using the developed microbial simulator. Effects of clogging and chemotaxis on microbial transport were simulated in a one-dimensional reservoir model. The feasibility of applying the microbial system for modifying injection profiles from a wellbore was investigated in a two-dimensional cross section model. Simulation of the relative permeability results demonstrated that microbial treatment could improve oil recovery over waterflooding alone.

DESCRIPTION OF MATHEMATICAL MODEL

Mathematical models for microbial transport processes were developed in two steps. The first step was to develop a mathematical model to predict the propagation and distribution of microorganisms and nutrients in porous media. This transport model accounts for physical phenomena that affect the transport of microbial systems such as diffusion, adsorption, growth and decay of microorganisms, and consumption of nutrients. Porosity reduction and permeability changes due to cell clogging have been considered in this model. This model can be used to predict the concentration distributions for injected nutrients and microorganisms with various injection modes at either field or laboratory scale.

The second step was to incorporate the transport equations for microorganisms and microbial nutrients into a three-dimensional, three-phase (oil, water, and gas) black oil simulator. The change of rock's wettability and associated relative permeability values after microbial treatments were accounted in the model for additional oil recovery. Distributions of pressure and oil/water/gas saturation in porous media were solved from the continuity equation. The Darcy flow velocity due to the pressure gradient in porous media was then used in the transport calculation for microorganisms and microbial nutrients. Using this simulator, the transport of microorganisms can be investigated, and the effect of a microbial system on oil recovery can be studied.

Transport Formulation

Microbial transport in porous media is described by the following equations:[5]

$$\vec{\nabla} \cdot \vec{\vec{D}} \cdot \vec{\nabla}(\phi SC) - \vec{\nabla} \cdot (\vec{u}C) - k_m \vec{\nabla} \cdot (C\vec{\nabla} \ln C_f) + \phi S(\mu - k_d)C + QC/V = \frac{\partial(\phi SC)}{\partial t} + \phi S k_c C - k_y \rho \sigma \left(\frac{\Omega}{\phi}\right)^h \quad (1)$$

where σ is solved from

$$\frac{\partial \sigma}{\partial t} = (\mu - k_d)\sigma + k_c \frac{\phi SC}{\rho} - k_y \sigma \left(\frac{\Omega}{\phi}\right)^h \quad (2)$$

The five terms on the left-hand side of Eq. 1 correspond to the dispersion, convection, chemotaxis, growth and decay, and injection/production of microbes, respectively. The right-hand side of Eq. 1 show the accumulation, clogging, and declogging of microbes in the aqueous phase. Equation 2 describes the growth, decay, clogging, and declogging of microbes on the rock surface.

The growth of microbes, μ, was assumed to follow the Monod equation:[13]

$$\mu = \frac{\mu_m C_f}{K_s + C_f} \quad (3)$$

where μ_m is the maximum growth rate achievable and K_s is that value of the concentration of the substrate where the specific growth rate has half its maximum value. Values of μ_m and K_s can be obtained from experimental results. The decay rate was assumed to be a first-order reaction.

The deposition of microbes is determined by clogging and declogging mechanisms as expressed in the last two terms in Eq. 1. The clogging rate is assumed to be proportional to the microbial concentration. The power term in the declogging term dictates the desorption rate of microbes as a function of adsorption saturation on the rock surface.[5] The chemotactic flow of microbes, which was induced by the presence of nutrients, was assumed to follow an exponential gradient of nutrient concentration.[5-6] The change of porosity of the porous medium was accounted by the deposition of microbes:

$$\phi = \phi_0 - \sigma \tag{4}$$

where ϕ_0 is the original porosity of the porous medium. The permeability reduction due to the deposition of microorganisms to the rock pore space was assumed to follow:[14]

$$\text{Log}(k) = a_0 + a_1 \cdot (\phi) \tag{5}$$

where a_0 and a_1 are experimentally determined constants.

The transport of nutrient is described by the following equation:[5]

$$\vec{\nabla} \cdot \vec{\vec{D}}_f \cdot \vec{\nabla} (\phi S C_f) - \vec{\nabla} \cdot (\vec{u} C_f) - \mu(\phi S C + \rho \sigma)/Y + Q C_f / V = \frac{\partial(\phi S C_f)}{\partial t} \tag{6}$$

Shown on the left-hand side of Eq. 6, the dispersion, convection, consumption, and injection/production terms of nutrient make up the nutrient transport equation in the aqueous phase. The yield coefficient Y is defined as the mass of cells produced per unit of substrate removed. Equation 1 is coupled with Eq. 6 in solving concentration distributions of microbes and nutrients.

The flux terms in transport Eqs. 1 and 6 are solved from three-dimensional, three-phase continuity equations applicable in an environment of black oil reservoirs.[15] The continuity equations are given by:

$$-\vec{\nabla} \cdot \left(\frac{\rho}{B}\vec{u}\right)_m - Q_m = \frac{\partial}{\partial t}\left(\frac{\phi \rho S}{B}\right)_m \tag{7}$$

where m = oil, water, or gas phase

Sources (injectors) and sinks (producers) at various strengths are assigned through well rates (Q) in the model. The gas produced from metabolism of a microbial system is taken into account in the model also through the term of Q in Eq. 7.

Oil Recovery Model

Microbial treatments recover additional oil from rock through alteration of relative permeability relationships and residual oil saturations in porous media. The reliable prediction of oil recovery in the MEOR process requires a proper model to represent these changes in the mathematical simulator based on comprehensive laboratory experiments.

The change of rock's wettability and associated relative permeability values after microbial treatments were demonstrated in laboratory tests. Relative permeability values associated with this microbial process are modeled in the numerical simulator as follows.

The rock wettability was found to vary with presence of microorganisms. Thus, the wettability change, ΔW, after microbial treatment is expressed as

$$\Delta W = b_0 + b_1 \ln [C_b] + b_2 (\ln [C_b])^2 \tag{8}$$

where the coefficients b_0, b_1, and b_2, are determined in the laboratory for a specific system of rock, oil, and microbes. The change of wettability alters the residual saturations in porous media. The associated residual oil saturation S_{or} and residual water saturation S_{wr} are determined from experiments for the same system and formulated as:

$$S_{or} = a_{o1} + a_{o2} W + a_{o3} W^2 \tag{9}$$

$$S_{wr} = a_{w1} + a_{w2} W + a_{w3} W^2 \tag{10}$$

where

$$W = W_0 + \Delta W \tag{11}$$

Experiments showed that microbial treatments caused a shift of wettability of siloxane-treated Berea sandstone cores from an oil-wet index (about – 0.8) to neutral-wet index (about – 0.2) as illustrated in Fig. 1. The wettability index values were measured in a centrifuge using the USBM method.[16] The associated S_{or} values decreased from about 0.25 to about 0.20. Coefficients of a_{o1}, a_{o2}, and a_{o3} in Eq. 9, determined from curve fitting of Fig. 1, are 0.177, 0.055, and 0.051 respectively, for the studied siloxane cores and microbial cells. The determined residual saturation values are then used to define the relative permeability (k_r) values for both oil and water phases. The following k_{ro} models are based on the concept of capillary number.

$$k_{ro} = k^{\circ}_{ro} \left(\frac{S_o - S_{wr}}{1 - S_{or} - S_{wr}} \right)^{e_c} \tag{12}$$

where

$$k^{\circ}_{ro} = k^{\circ}_{row} + \frac{S_{orw} - S_{or}}{S_{orw}} (k^{\circ}_{roc} - k^{\circ}_{row}) \tag{13}$$

$$e_o = e_{ow} + \frac{S_{orw} - S_{or}}{S_{orw}} (e_{oc} - e_{ow}) \tag{14}$$

A relative permeability model similar to that of Eqs. 12, 13, and 14 can also be formulated for the water phase. Thus, the relative permeability value determines the proportional flow of the oil phase in the presence of microbial cells and the amount of additional oil recovery from porous media.

Numerical Solution

The fluid flow Eq. 7 is solved for Darcy velocity using an IMPES procedure. A no-flow boundary of the reservoir is implemented by setting the pressure gradient at boundary interfaces to zero. This is followed by the solution of transport equations of microbes (Eq. 1) and nutrients (Eq. 6). The Crank-Nicolson method[17] was used in formulating the finite difference form of transport equations. Both microbial and nutrient concentrations were solved implicitly in space using a direct solution method for the sparse matrix. The amount of deposition of microorganism was then calculated, and the permeability was adjusted for pressure calculations in the next time step.

EXPERIMENTAL APPARATUS, PROCEDURES, AND RESULTS

Laboratory experiments were conducted with microbial isolates that produce mainly gases and surfactants when fermenting sugars such as those present in molasses. Unsteady-state relative

permeability measurements were conducted using a surfactant-producing microorganism. CT imaging experiments using microorganisms were conducted to evaluate the production of gas inside a Berea sandstone core and determine the effects of trapped gas saturation on improved oil recovery by microbial formulations. Results from microbial coreflooding experiments were used to determine microbial transport parameters for the simulator.

Coreflood Apparatus and Procedures

Unfired Berea sandstone cores were used in these studies. Core preparation and the experimental equipment used have been described previously.[18]

Crude Oil

Crude oil samples were obtained from the Bartlesville sand in Delaware-Childers and Chelsea-Alluwe fields in northeastern Oklahoma. Delaware-Childers oil has a gravity of 31° API [0.87 g/cm^3] and a viscosity of 7.5 cP at 77 °F; Chelsea-Alluwe oil has a gravity of 34° API [0.85 g/cm^3] and a viscosity of 8.1 cP at 77 °F. The mineral oil used in the relative permeability experiments had a viscosity of 46 cP at 77 °F.

Microorganisms

Results from previous studies have shown that a combination of an adapted strain of *Bacillus licheniformis*, NIPER 1A (ATCC No. 39307) and a *Clostridium* species, designated as NIPER 6, was the most effective formulation for oil recovery in porous media. These strains have been described elsewhere.[18] NIPER 7 is another species of *Clostridium* that produces a greater quantity of carbon dioxide than NIPER 6 when fermenting sucrose in molasses.

Chemicals and Media

The molasses used in these experiments was obtained from Pacific Molasses Company in Oklahoma City, OK. Its composition has previously been described.[18] The concentration of molasses used in these experiments was 4% vol/vol in tap water with 0.1% wt/vol ammonium phosphate added.

Unsteady-State Relative Permeability Tests

Cores that had been brine flooded (3% by weight potassium chloride (KCl)) were then aged in crude oil for 1 week, and the crude oil was displaced dynamically with mineral oil. The core was immediately waterflooded with either 3% KCl brine or the microbial formulation. The cores were waterflooded at a constant pressure calculated from a theoretical flow rate of 0.1 cm^3/sec (113.7 ft/d) to overcome end effects. The brine (or microbial formulation) was injected at constant pressure, and water and oil volumes produced were measured as a function of time. These data were used to calculate relative permeability values for water and oil using the method of Johnson, Bossler and Naumann.[19]

CT Imaging

The dynamics of fluid flow and microbial gas production were investigated using rock-fluid imaging techniques. Displacement experiments were monitored using X-ray computed tomography (CT scanning) to determine gas production and its effects on fluid flow. A Siemens Somatom II computed tomography (CT) scanner was used to obtain images of cores. Detailed information about the use of these techniques has previously been presented.[20] No tagging

techniques were used unless oil was present. When crude oil was used, it was tagged with 20 or 30% iododecane.

Experimental Results

Microbial Retention Tests

Coreflood experiments were conducted to obtain information on microbial transport in 0.83 ft-long (25.3 cm) Berea sandstone core samples for incorporation in the numerical model. Microorganism NIPER 6 was used for all retention tests. The cores were saturated with 0.5% NaCl brine. NIPER 6 microbial cells were grown up to a concentration of at least 1 x 10^7 cells/mL. Tracer was injected and the effluent collected to determine the retention of Tracer 1. The cells were then centrifuged, washed, and injected. The effluent was collected and the microbial retention was then determined. Tracer was again injected and the effluent collected to determine the retention of Tracer 2. It is believed that after an initial adsorption of microbes on pore surfaces, a point would be reached at which all irreversible sites of adsorption would be saturated and cell transport and recovery would increase with subsequent injection of microbes. Volumes of the microbial formulation (washed cells without nutrient) were injected into core samples at a rate of 0.5 cm^3/min (approximately 10 ft/d) and the microbial concentration in the core effluent was determined. Subsequent cores had increasing injection slug sizes. Microbial concentrations were monitored using selective media. Before and after each microbial injection, a tracer injection was performed to see if adsorption of microbes caused any alteration in the interstitial velocity. The interstitial velocity of all tracer injections was about 0.078 cm/min, or 3.7 ft/d. These velocities did not change after microbial injection. A linear correlation was obtained between the amount of microbes injected and the amount of microbes recovered (Fig. 2). In contrast to significant microbial retention in Berea sandstone cores, more than 95% of injected tracers were recovered in a majority of the retention tests. Simulation matches have been completed for microbial transport in the cores that had 0.75, 1.0, 1.25, and 1.5 PV injected.[21]

Pressure Profile

Pressure profiles from several microbial corefloods (0.83 ft-long; 25.3 cm) were monitored in the laboratory. In the coreflood test, 0.1 pore volume (PV) of microbial solution was introduced into the core. This was followed by an injection of 0.2 PV of nutrient solution and 3 days of shut-in. After the shut-in, another 0.2 PV of nutrient solution was injected and followed by waterflood at 1 ft/day. The profiles of pressure drop across several corefloods during the brine injection are shown in Fig. 3. Results from coreflooding experiments have shown pore plugging and production of biogenic gas by the microorganisms. The pore plugging decreases the rock permeability, and the creation of the gas phase reduces the relative permeability of the water phase. A numerical simulation match of the pressure profiles from two of these microbial corefloods (cores M-91 and M-92) is also presented in Fig. 3. The mathematical model matches the pressure changes of corefloods M-91 and M-92 reasonably well. Table 1 lists the parameters used to match these corefloods.

Unsteady-State Relative Permeability Tests

Relative permeability measurements were conducted on adjacent samples from two sets of Berea sandstone that had different permeability ranges. Each set includes one sample with brine-oil relative permeability and another sample used for NIPER 1A-oil relative permeability tests. A summary of the results is presented in Table 2. The two samples from each group are presented together graphically for comparison studies. Comparisons of the relative permeability fraction curves and ratio curves have been published previously.[18] A higher relative permeability to oil was apparent in both microbially flooded samples as compared to brine-flooded samples. The

higher permeability core exhibited the effect much earlier in the flood. Sample R2 exhibited a significant decrease in relative permeability to water throughout the flood. This higher permeability core, flooded with a microbial formulation that had been incubated 24 hours, exhibited an increase in oil production and relative permeability to oil immediately and continuing throughout the flood.

Oil recovery before water breakthrough was derived from the fractional flow equations using the viscosity of the Delaware-Childers oil. The samples waterflooded with the microbial formulation had a higher oil recovery before water breakthrough. A greater difference was observed in the relative permeability characteristics for the higher permeability sample that had been flooded with the 24 hr microbial culture. A significant decrease was seen in k_{rw} curves (a decrease in water mobility) for two of three samples containing microbial formulation. Both relative permeability test samples showed an increase in relative permeability to oil. A slight shift to the right was observed at the brine saturation at which oil and water relative permeabilities are equal (crossover). Samples tested with the microbial formulation had higher oil recovery before water breakthrough and lower residual oil saturations.

CT Imaging Experiments

A CT imaging experiment using microbes in Berea sandstone was conducted to determine if gas production by microorganisms could be distinguished in a core. A brine-saturated core was injected with 1 PV of NIPER 7, one of the better gas producers from NIPER's microbial culture collection. The core was then scanned to determine if the gas could be observed, and the saturations of liquid and gas determined. Reconstruction of the CT images showed a surprising amount of gas in the core (Fig. 4). When the densities were calculated, there was a total gas saturation of 18.4% in the core.

This experiment was repeated using Chelsea-Alluwe crude oil tagged with 30% iododecane. The core was waterflooded to residual oil saturation and then injected with 0.1 PV of NIPER 7 and 0.4 PV of 4% molasses. The core was then incubated for 48 hr and the pressure was monitored. Figure 5 shows the image of the core after the waterflood to residual oil saturation (S_{orwf}) and during the waterflood after microbial treatment. The saturations of this core were as follows: (1) Initial oil saturation (S_{oi}) - 57.5%; (2) Oil saturation after waterflood (S_{orwf}) - 33.6%; and (3) Oil saturation after incubation during the second waterflood (S_{ormf}) - 29.7%. During microbial incubation the pressure rose to 39 psi. This particular gas-producing microbial injection gave a recovery efficiency (E_r) of 11.6%.

SIMULATION OF COREFLOOD EXPERIMENTS

Parameters of the microbial transport system were determined from laboratory experiments or from simulation matches of laboratory tests using the developed mathematical model. The laboratory experiments included microbial coreflood tests and flask tests.

Figure 6 shows the microbial growth and nutrient consumption from a flask test. The population of the microbial system used, designated NIPER 6, grew to 10^6 times within 20 hours with a full supply of nutrients in a flask. This is equivalent to a maximum growth rate of 8.4 day^{-1}. The decay rate constant, determined from the population change during the period of 200 to 600 hours in Fig. 7, is 0.22 day^{-1}. The cell yield coefficient, Y, of 0.5 was computed from the nutrient consumption rate.

To determine model parameters, mathematical simulations were performed to match coreflood tests of diffusion, adsorption, concentration profiles, and pressure profiles. The core model was dimensioned at 50 * 1 * 1 in simulation runs. The relative permeability values were determined

from a microbial coreflood in the laboratory.[18] Table 3 lists several microbial system parameters used in the following laboratory and field scale simulations.

Diffusion

A tracer coreflood test was matched in Fig. 7 using a diffusion coefficient of 8.93E-5 cm^2/sec or 8.3E-3 ft^2/day. A total of 0.2 pore volume of 50 ppm fluorescein tracer was injected into the 4-ft Berea sandstone core at a rate of 0.73 ft/day. More than 99% of tracer was recovered from this coreflood test.

Adsorption

The concentration profiles of microbial coreflood effluents were matched for a total of four coreflood tests to determine clogging and declogging rate constants. In the four coreflood tests, microbes were introduced at four different pore volumes: 0.25, 0.75, 1.0, and 1.5, respectively. Virtually no microbes were recovered in the coreflood effluent at a microbial injection of 0.25 pore volume. The microbial concentration in the effluents increased with the increase of microbial injection from 0.75 to 1.5 pore volumes. These tests showed an irreversible clogging or adsorption until 0.3% bulk volumes of pore space were deposited by microbes. Values of 25 and 37 day^{-1} were determined for clogging and declogging rates, respectively, from matches of microbial effluents of four coreflood tests. Figures 8a through 8c show these simulation matches for experimental injections of 0.75, 1.0, and 1.5 pore volumes of microbes, respectively. Input parameters for matching the coreflood test that used 1.5 pore volumes of microbial injection are listed in Table 4.

Microbial Concentration Profile

One microbial/nutrient coreflood experiment was conducted in a 4-ft-long (122 cm) core. The core was injected with 0.05 pore volume of nutrient (4 wt % molasses) followed by injections of 0.1 pore volume of microbes and 0.05 pore volume of nutrient. The core was then incubated (shut-in) for 3 days and injected with 0.1 pore volume of nutrient. The core was shut in for another 3 days before the initiation of waterflood. The microbial concentrations were monitored from the four ports which were 0.5 ft (15.2 cm), 1.5 ft (45.7 cm), 2.5 ft (76.2 cm), and 3.8 ft (115.8 cm), respectively, from the injection end of the core. Figures 9a and 9b show the simulation results of microbial and nutrient concentrations at 0.5 pore volume of waterflood. The core properties and microbial/nutrient parameters are listed in Table 5.

Pressure Profile

A pressure profile from a microbial coreflood test was matched in the simulation run. In the coreflood test, 0.1 pore volume of microbial solution was introduced into the core. This was followed by an injection of 0.2 pore volume of nutrient solution and 3 days of shut-in. After the shut-in, another 0.2 pore volume of nutrient solution was injected and followed by waterflood at 1 ft/day (30.5 cm/day). The profile of pressure drop across the core during the brine injection was monitored and is shown in Fig. 10, together with the modeling match and the calculated profile of porosity change due to clogging and declogging reactions. A published value[14] of 25.2 for the permeability-porosity coefficient a_1 in Eq. 5 was used in the model to account for the permeability reduction caused by microbial deposition. A biogenic gas production rate of 30 mL per gram of nutrient consumption, which was measured from a separate test, was used in the simulation. Table 6 lists values of parameters used in the simulation match.

The initial pressure drop during waterflooding before the microbial treatment was 1.5 psi. The simulation results showed that the sharp increase of pressure drop after the microbial flooding

is caused by pore plugging and the production of biogenic gas. The pore plugging reduces the rock permeability and the increase of gas saturation decreases the relative permeability of the water phase. As the waterflood proceeds, the permeability (or porosity) recovers slightly (Fig. 10) with the declogging of microbes in the pore space; therefore, a drop in pressure gradient was observed from the coreflood.

FIELD-SCALE SIMULATIONS

Field-scale simulation runs were conducted to study the microbial transport in reservoirs using the developed microbial simulator. Effects of clogging and chemotaxis on microbial transport were simulated in a one-dimensional reservoir model. The feasibility of applying the microbial system for modifying injection profiles from a wellbore was investigated in a two-dimensional cross section model. Table 7 shows the reservoir model and the microbial parameters used in simulations. In the one-dimensional simulation run, only the top layer was used as the reservoir model. Injection rates used were 100 bbl/day in the one-dimensional simulation runs and 300 bbl/day in the two-dimensional simulation runs. Injection sequence and sizes of the slugs in each simulation run are shown in the figures 11 through 14.

The clogging or adsorption of microorganisms to the rock surface was found to be critical to the transport of microbes in reservoirs from simulation results. Figure 11 shows concentration profiles of microbes in formations with three different clogging parameters: 0, 1, and 25 day^{-1}, respectively. The microbial slug penetrates 70 ft (2.1 m) into the formation when the clogging reaction is absent or k_c is equal to 0. The penetration depth of microbes is reduced to 30 ft ((0.91 m) when k_c is 1 day^{-1} and a much smaller microbial slug is found to move away from the wellbore when k_c is increased to 25 day^{-1} due to loss of microorganisms to the rock surface.

The effect of chemotaxis on the microbial transport is shown in Fig. 12. The microbial concentration profiles, simulated at three different values of chemotaxis coefficients (k_m): 0, 1, and 3, respectively, were plotted together with the profile of the nutrient concentration. Because of the high concentration of nutrient close to the injection wellbore, a higher concentration of microbes is found close to the injector for microbes with a higher value of k_m than those with lower values of k_m. At a distance of 10 ft (0.31 m) or deeper into the formation, on the other hand, a higher concentration is found for microbes with lower values of k_m. For the case studied, the microbial concentration for a k_m value of 0 is about three times as much as those with a k_m value of 3 when the distance is more than 20 ft (0.61 m) away from the injector.

Simulations of injection profile modification using microbial treatments were run on a two-layer cross section model. The top layer has a permeability of 1000 md and pay thickness of 20 ft (0.61 m) whereas the bottom layer has a permeability of 100 mD and pay thickness of 10 ft. Five feet in the x-direction was used as the size for wellbore grids and grids next to the injection wellbore. The microbes and nutrients were introduced into the injection well in the model after water breakthrough from the high-permeability layer. The plugging of microorganisms to the wellbore next to the high-permeability layer diverts the injection water into the low-permeability layer (Fig. 13). Compared to the case without microbial treatment, this results in a decrease of water-oil-ratio (Fig. 14) and, therefore, an increase of oil recovery during the waterflood. The clogging and declogging rate constants were assumed to be 25 and 37 day^{-1}, respectively, in models. The fractional injection of water into the low-permeability layer drops during the later stage of waterflood due to microbial declogging and the cease of nutrient injection. These simulation runs support the feasibility of applying microbial treatments to improve the injection profile in waterfloods.

Simulations were performed to study the effect of selective layer treatment in the microbial profile modification. The microbes were injected only into the high-permeability layer in the case

of single-layer treatment. The selective treatment of the high-permeability layer is more effective in diverting the injected water into the low-permeability layer (Fig. 13). Figure 14 shows the comparison of oil recovery from a two-layer treatment and a single-layer treatment. More oil is recovered with the single-layer treatment.

Numerical simulations at a field scale were conducted to estimate additional oil recoveries resulting from changes in relative permeabilities after microbial treatments. Microbial injections followed by waterfloods were simulated in a quarter of a five-spot well pattern. The two-dimensional reservoir models were dimensioned at 30 grids in both the x and y directions. Relative permeability measurements obtained from test R2 (table 3) were used in microbial flood simulations. Other reservoir parameters and fluid properties used in simulations are listed in Table 8. Remaining oil saturations before microbial waterfloods were assumed to be 30, 35, and 45%, respectively, in three sets of simulations for investigating the effect of the microbial flood on reservoirs of different oil saturations. For comparison of oil recoveries, waterfloods were simulated at three oil saturations, respectively, based on the same reservoir model except that relative permeability values measured from the R1 brine test were used. Figure 15 shows oil recoveries predicted by numerical simulations of waterfloods and microbial floods. Based on relative permeability values from R1 and R2 tests, the microbial flood recovers an additional 2.0, 3.9, and 5.1% pore volumes of oil, respectively, over waterfloods for reservoirs containing remaining oil saturations of 30, 35, and 45%. This shift of relative permeability end points to smaller values of residual oil saturation after microbial treatments, results in additional oil recovery from reservoirs.

CONCLUSIONS

The following conclusions were drawn from this study:

1. A three-dimensional, three-phase, multiple-component simulator that includes all required mechanisms and transport phenomena of microbial systems in porous media can be used to predict the propagation of microbes and nutrients in the porous media to design laboratory experiments and field operations in order to optimize injection strategies for improving oil recovery.

2. Laboratory experiments were successful in determining input parameters of the microbial system for the developed mathematical model, and progress has been made towards incorporating microbial oil recovery mechanisms into the model.

3. The simulator can be used to study the effects of adsorption, chemotaxis, and injection strategy on the transport process of the microbial system in the porous media. Clogging or adsorption of microbes to a rock surface is critical to the transport of microorganisms in porous media.

4. Simulation of the relative permeability results demonstrated that microbial treatment could improve oil recovery over waterflooding alone.

5. CT imaging was used successfully to calculate microbial gas saturation in Berea sandstone, and improved our understanding of the contributions of microbial gas production to oil recovery. Gas production by microorganisms decreases residual oil saturation after waterflooding in porous media.

ACKNOWLEDGMENTS

This work was supported by the U. S. Department of Energy under Cooperative Agreement DE-FC22-83FE60149. Dr. Fred W. Burtch and Rhonda Patterson of the DOE Bartlesville Project Office are acknowledged for their help in conducting this work. The authors thank Drs. Liviu Tomutsa and Bonnie Gall for their assistance in computerized tomography experiments.

NOMENCLATURE

a_{o1}, a_{o2}, a_{o3} = experimentally determined constants for Eq. (2)

a_{w1}, a_{w2}, a_{w3} = experimentally determined constants for Eq. (3)

b_0, b_1, b_2 = experimentally determined constants for Eq. (1)

C= microbial concentration, gm/mL or cells/mL

C_f= nutrient concentration, gm/mL

$\vec{\vec{D}}$ = effective dispersion coefficient tensor for microbes

$\vec{\vec{D}}_f$= dispersion coefficient tensor for nutrient

E_r= recovery efficiency, $\frac{S_{orwf} - S_{ormf}}{S_{o\ldots}} \times 100\%$

e_o = exponent parameter of relative permeability in oil phase

e_{oc} = exponent parameter of relative permeability in oil phase at high capillary number

e_{ow} = exponent parameter of relative permeability in oil phase at low capillary number

Q = well rate, stb/day or mL/sec

S = aqueous saturation

V = bulk volume of well block, ft^3 or mL

h = declogging parameter

k = permeability, md

k_o= initial permeability, md

k_{rw}= relative permeability to water, md

k_{rw}/k_{ro}= relative permeability fraction

k_r = relative permeability

k_{ro} = relative permeability of oil phase

k^o_{roc} = relative permeability of oil phase at high capillary number

k^o_{row} = relative permeability of oil phase at low capillary number

k_m= chemotaxis coefficient

k_d = decay rate, day^{-1}

k_c = clogging rate, day^{-1}

k_y = declogging rate, day^{-1}

S_{oi}= initial oil saturation, percent pore volume (%PV)

S_{orwf} = oil saturation after waterflooding, %PV

S_{ormf} = oil saturation after microbial treatment and subsequent waterflood, %PV

S_o = oil saturation

S_{or} = residual oil saturation

S_{wr} = residual water saturation

S_{orw} = residual water saturation at low capillary number

u = Darcy velocity, cm/sec or ft/day

W = wettability index

W_o = original wettability index

ΔW = alteration of wettability index

Y= yield coefficient

ρ= microbial density, gm/mL or lb/ft^3

μ= growth rate, day^{-1}

ϕ= porosity

σ= volume of deposited microbes / volume of porous medium

REFERENCES

1. NIPER Annual Research Plan for FY92.

2. Bryant, R. S. and T. E. Burchfield, Review of Microbial Technology for Improving Oil Recovery, SPE Reservoir Engineering, May 1989, pp. 151-154.

3. Bryant, R. S. and J. Douglas, Evaluation of Microbial Systems in Porous Media for EOR, SPE Reservoir Engineering, May 1988, pp. 489-495.

4. Hitzman, D. O. Review of Microbial Enhanced Oil Recovery Field Tests, Proceedings of the Symposium on Applications of Microorganisms to Petroleum Technology, NIPER-351, DE88001232, September, 1988.

5. Corapcioglu, M. Y. and A. Haridas. Transport and Fate of Microorganisms in Porous Media: A Theoretical Investigation. J. of Hydrology, v. 72, 1984, pp 149-169.

6. Dahlquist, F. W., P. Lovely, and D. E. Koshland, Jr. Quantitative Analysis of Bacterial Migration in Chemotaxis. Nature New Biology, v. 236, March 1972, pp 120-123.

7. Tien, C. and S. Wang. Dynamics of Adsorption Column with Bacterial Growth Outside Adsorbents, The Canadian J. of Chemical Engineering, v. 60, 363-376, June, 1982.

8. Kalish, P. J., J. A. Stewart, W. F. Rogers, and E. O. Bennett. The Effect of Bacteria on Sandstone Permeability, J. of Petroleum Technology, v. 16, 805-814.

9. Jang, L., M. M. Sharma, and T. F. Yen. The Transport of Bacteria in Porous Media and Its Significance in Microbial Enhanced Oil Recovery. Pres. at the 1984 SPE California Regional Meeting in Long Beach, CA, April 11-13. SPE 12770.

10. Sarkar, A. K., M. M. Sharma, and G. Georgiou. Compositional Numerical Simulation of MEOR Processes. Development in Petroleum Science v. 31, paper no. R-21, Pres. at 1990 International Conference on Microbially Enhanced Oil Recovery, May 27 - June 1, 1990.

11. Islam, M. R. Mathematical Modeling of Microbial Enhanced Oil Recovery. Pres. at the 65th SPE Annual Conference at New Orleans, LA, September 23-26, 1990. SPE 20480.

12. Knapp, R. M. and F. Civan. Modeling Growth and Transport of Microorganism in Porous Formations. Pres. at 1988 Meeting of International Association for Mathematics and Computers in Simulation at Paris, France.

13. Gaudy, A. F. Jr. and E. T. Gaudy. *Microbiology for Environmental Scientists and Engineers*, McGraw-Hill Book Co., 1980.

14. Chilingarian, G. V., J. Chang, and K. I. Bagrintseva. Emperical Expression of Permeability in terms of Porosity, Specific Surface Area, and Residual Water Saturation of Carbonate Rocks. J. of Petroleum Science and Engineering, vol. 4, pp. 317-322, 1990.

15. Fanchi, J. R., K. J. Harpole, S. W. Bujnowski, and H. B. Carroll, Jr. BOAST: A Three Dimensional, Three-Phase Black Oil Applied Simulation Tool (Version 1.1). Volume I: Technical Description and Fortran Code. U. S. Dept. of Energy Report No. DOE/BC/10033-33, v. 1., Sept. 1982.

16. Lorenz, P. B., Donaldson, E. C., and Thomas, R. D.; "Use of centrifugal Measurements of Wettability to Predict Oil Recovery," U.S. Bureau of Mines, Bartlesville Energy Technology Center, Report 7873, 1974.

17. Von Rosenberg, D. U. *Methods for Numerical Solution of Partial Differential Equations.* Elsevier, New York, N.Y., 1977. p. 56.

18. Chase, K.L., R.S. Bryant, T.E. Burchfield, K.M. Bertus, and A.K. Stepp. Investigation of Microbial Mechanisms for Oil Mobilization in Porous Media. Development in Petroleum Science v. 31, paper no. R-4, Pres. at 1990 International Conference on Microbially Enhanced Oil Recovery, May 27 - June 1, 1990.

19. Johnson, E. F., Bossler, D. P., and Naumann, V. O. Calculation of Relative Permeability from Displacement Experiments, *Trans*, AIME, January, 1959.

20. Tomutsa, L., D. Doughty, S. Mahmood, A. Brinkmeyer, and M.P. Madden. Imaging Techniques Applied to the Study of Fluids in Porous Media. Report for the U.S. Department of Energy, NIPER 485, August, 1990.

21. Chang, M.-M., F. T. H. Chung, R.S. Bryant, H.W. Gao, and T E. Burchfield. Modeling and Laboratory Investigation of Microbial Transport Phenomena in Porous Media. SPE paper No. 22845, Pres. at the SPE Ann. Technical Meeting Oct. 6-8, 1991, Dallas, TX.

Table 1. Core properties and microbial system parameters used in matching pressure drop in a microbial coreflood

Parameter	Value
Core:	
length, ft, (cm)	0.912 (27.8)
diameter, ft, cm	0.125 (3.8)
Porosity, %	21.36
Permeability, mD	326
Injected microbial conc., cells/mL	5×10^8
Injected nutrient conc., lb/cu ft	2.5
Injection rate, ft/day, cm/day	1, 30.5
Permeability - porosity coefficient[1]	25.2
Gas production - ft^3/lb of nutrient	0.50

[1] See reference 10.

Table 2. Summary of unsteady-state relative permeability tests

			Initial Conditions	
Sample[1]	Permeability to air, mD	Porosity, percent	Water saturation, percent PV	Effective permeability to mineral oil, mD
R1	981	22.6	30.5	650[2]
R2	1240	22.8	30.4	837[3]
R7	322	18.9	25.3	209[2]
R8	323	19.0	25.8	202[4]

	Terminal Conditions		Oil Recovered		
Sample	Oil saturation, % PV	Effective k to water, mD	Percent PV	Percent OIP[5]	Before water breakthrough[6]
R1	30.3	127	39.3	56.5	23.5
R2	24.7	107	44.9	64.4	31.6
R7	32.2	17	42.5	56.9	26.7
R8	28.2	19	46.0	62.0	28.2

[1]All cores were aged for 1 week with Delaware-Childers oil.
[2]Brine/oil (mineral oil) relative permeability.
[3]24-hour microbial solution/oil (mineral oil) relative permeability.
[4]5-day oid microbial solution (optimal biosurfactant production)/oil (mineral oil) relative permeability.
[5]OIP = Oil in place.
[6]Calculated using oil viscosity of Delaware Childers oil.

TABLE 3. Microbial system parameters used in simulations

Diffusion coefficient	
microbes, ft^2/day	0.0055
nutrient, ft^2/day	0.0083
Declogging rate constant, day^{-1}	37.
Declogging parameter	0
Cell yield coefficient (Y)	0.5
Monod half growth constant, lb/cu ft	0.5
Maximum growth rate, day^{-1}	8.4
Decay rate, day^{-1}	0.22
Chemotaxis coefficient	0

TABLE 4. Core properties and microbial system parameters used in matching microbial effluent profiles

Parameter	Value
Core:	
length, ft, (cm)	0.833 (25.4)
diameter, ft, (cm)	0.125 (3.8)
Porosity, %	22.95
Permeability, mD	821
Injected microbial conc., cells/mL	5×10^8
Injected nutrient conc., lb/cu ft	0
Injection rate, ft/day, (cm/day)	1 (30.5)

TABLE 5. Core properties and microbial system parameters used in simulating microbial and nutrient concentration profiles

Parameter	Value
Core:	
length, ft, (m)	4.0 (1.2)
diameter, ft, (cm)	0.167 (5.1)
Porosity, %	17.1
Permeability, mD	64.8
Initial oil saturation, %	28.8
Initial water saturation, %	71.2
Injected microbial conc., cells/mL	5×10^8
Injected nutrient conc., lb/cu ft	2.5
Injection rate, ft/day, (cm/day)	1 (30.5)

TABLE 6. Core properties and microbial system parameters used in matching pressure drop in microbial coreflood

Parameter	Value
Core:	
length, ft, (cm)	0.912 (27.8)
diameter, ft, (cm)	0.125 (3.8)
Porosity, %	21.36
Permeability, mD	326
Injected microbial conc., cells/mL	5×10^8
Injected nutrient conc., lb/cu ft	2.5
Injection rate, ft/day, (cm/day)	1 (30.5)
Permeability - porosity coefficient	25.2
Gas production per lb of nutrient, cu ft	0.50

TABLE 7. Reservoir model and microbial system parameters used in field-scale simulations

Parameter	Value
Reservoir:	
length, ft, (m)	200 (61)
width, ft, (m)	200 (61)
thickness (top/bottom layers), ft (m)	20 and 10 (0.61 and 0.31)
Porosity, %	20
Permeability:	
k_x, k_y, k_z (top layer), md	100, 100, 10
k_x, k_y, k_z (bottom layer), md	1,000, 1,000, 100
Initial oil saturation, %	75
Initial water saturation, %	25
Injected microbial conc., cells/mL	5×10^8
Injected nutrient conc., lb/cu ft	2.5

Table 8. Reservoir and fluid parameters used in numerical field simulations

Parameters	Value
Reservoir:	
length, ft, (m)	330 (100.6)
width, ft, (m)	330 (100.6)
thickness, ft, (m)	30 (9.1)
depth, ft, (m)	600 (183)
Porosity, %	20
Permeability, md	1,000
Viscosity, cP	
oil	5
water	1
Initial saturations (oil/water/gas), %:	
case 1	30, 70, 0
case 2	35, 65, 0
case 3	45, 55, 0
Injection/production rate, stb/d	100

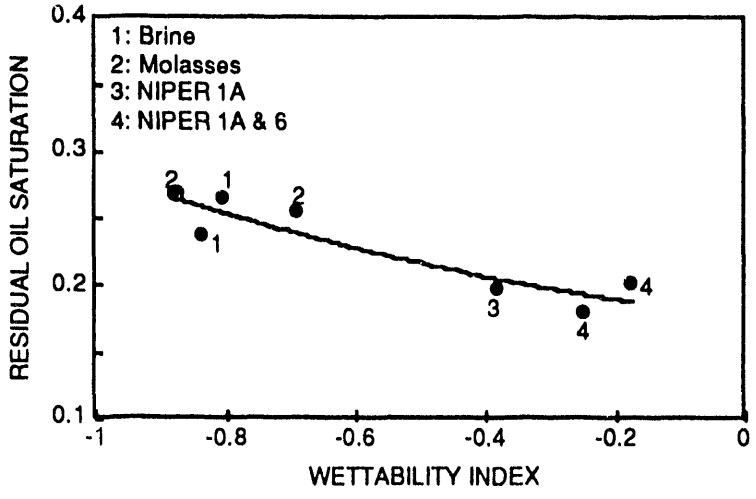

FIGURE 1. – Shift of wettability of siloxane-treated cores after microbial treatments.

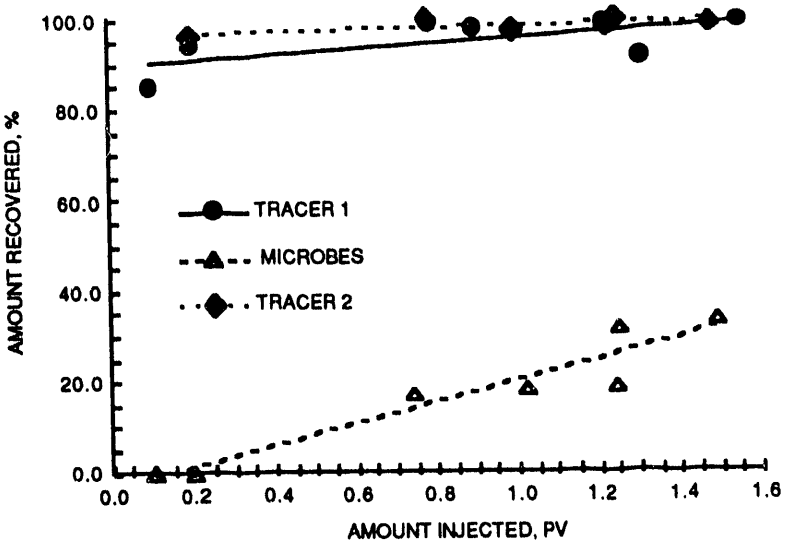

FIGURE 2. – Recovery of microorganisms vs. amount injected in coreflood experiments.

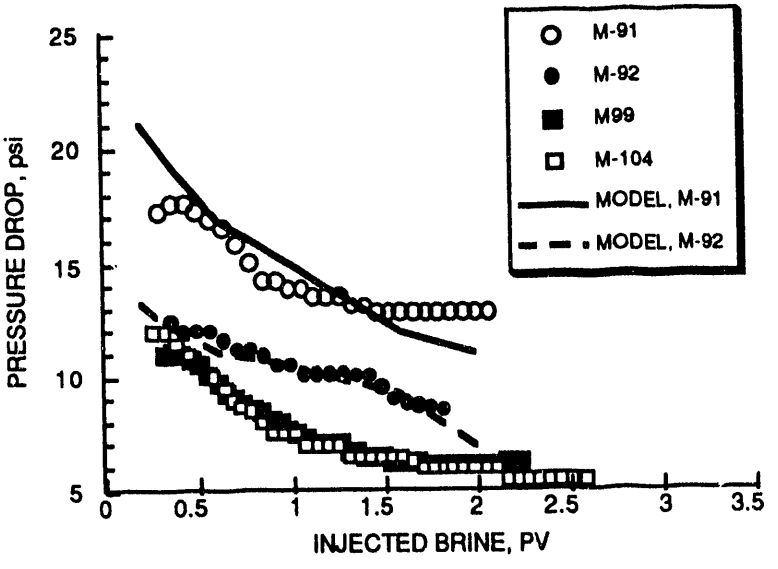

FIGURE 3. – Pressure drops during microbial corefloods, and simulation matches.

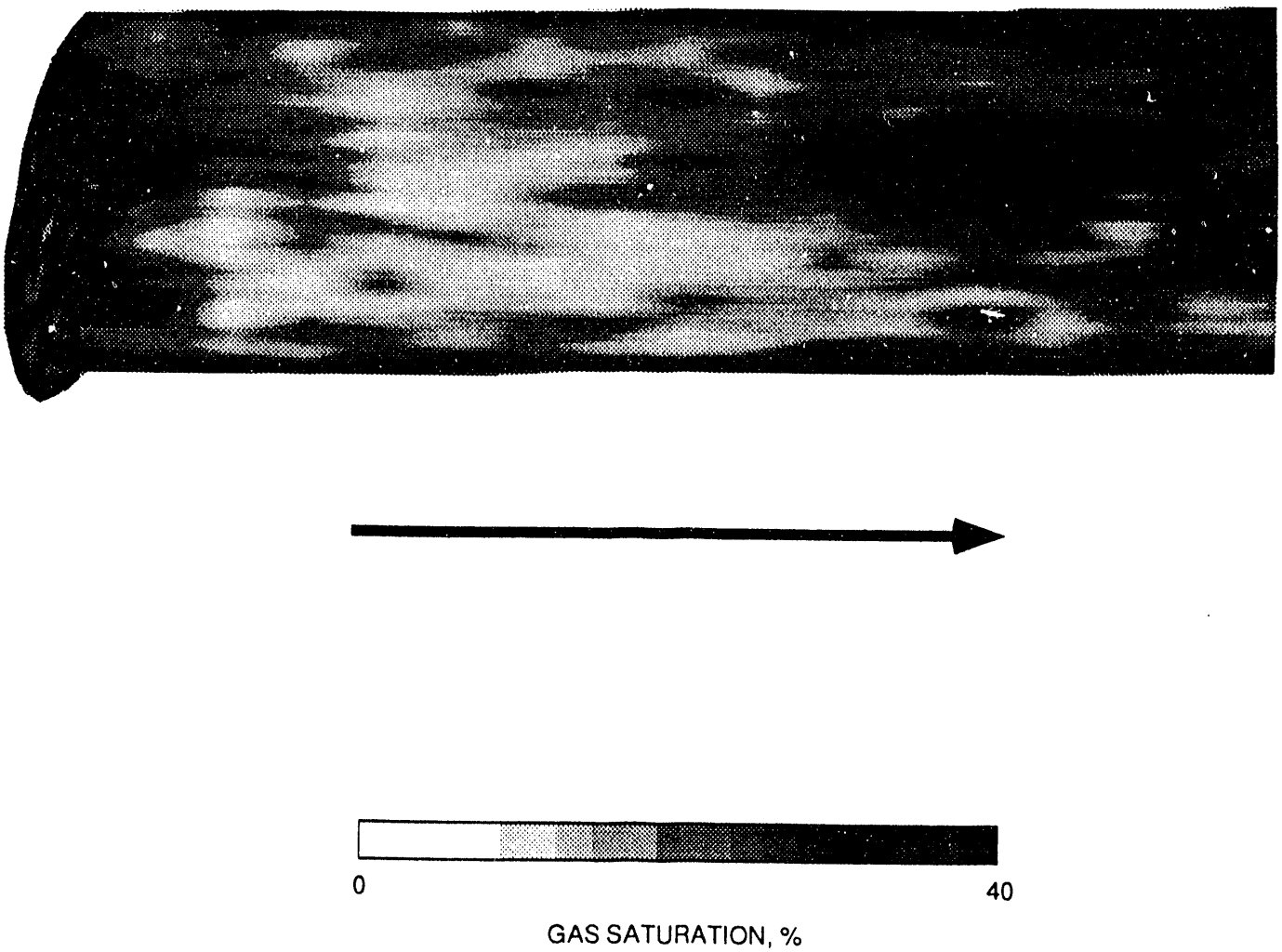

FIGURE 4. – CT image of core after microbial treatment showing gas saturation.

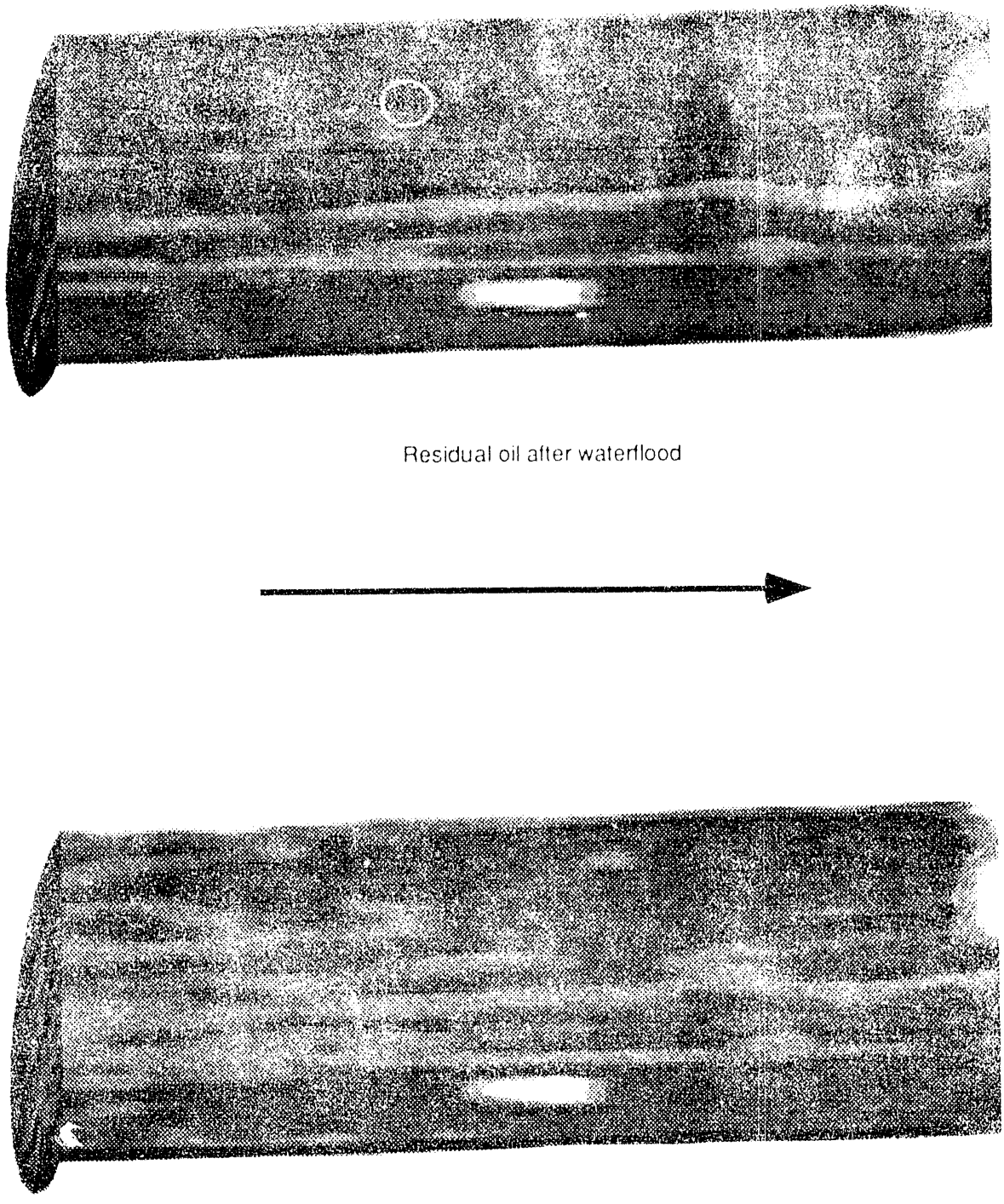

FIGURE 5. – CT image of core at residual oil saturation after waterflooding and core after microbial treatment and subsequent waterflooding.

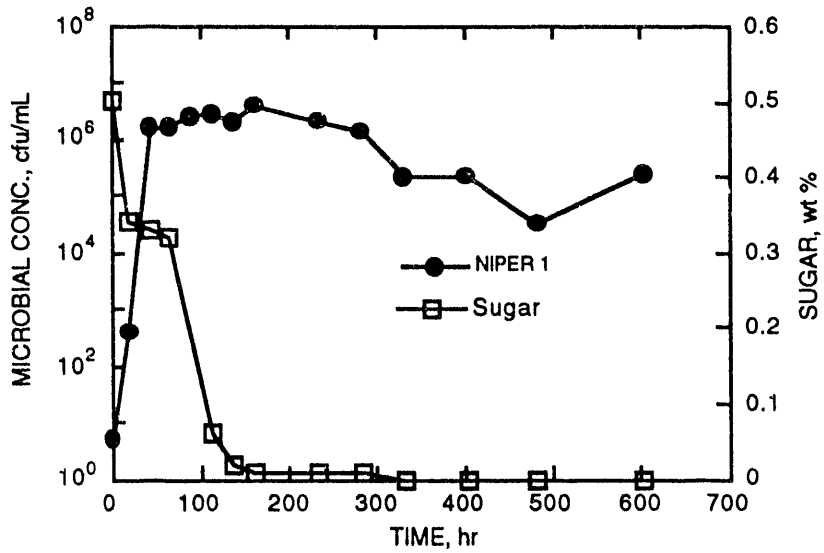

FIGURE 6. – Microbial concentration and sugar consumption in a flask test.

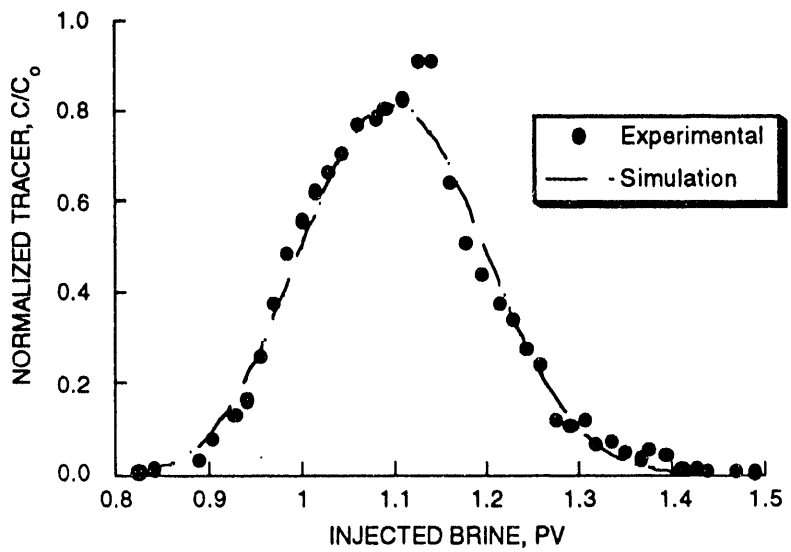

FIGURE 7. – Simulation match of experimental tracer data in a 4-ft long Berea sandstone core.

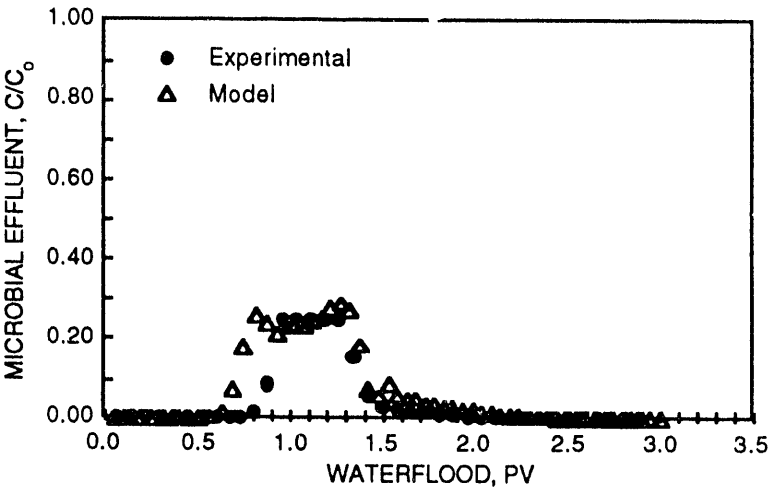

FIGURE 8a. – Simulation match of the microbial concentration in coreflood effluent after 0.75 PV injection.

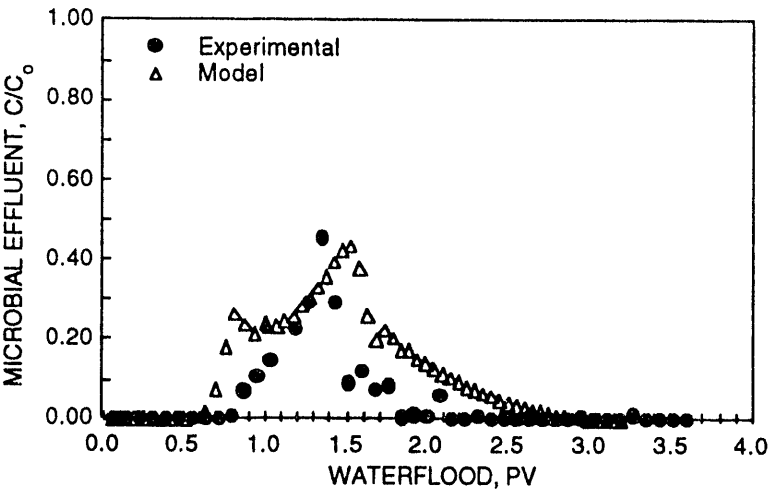

FIGURE 8b. – Simulation match of the microbial concentration in coreflood effluent after 1.0 PV injection.

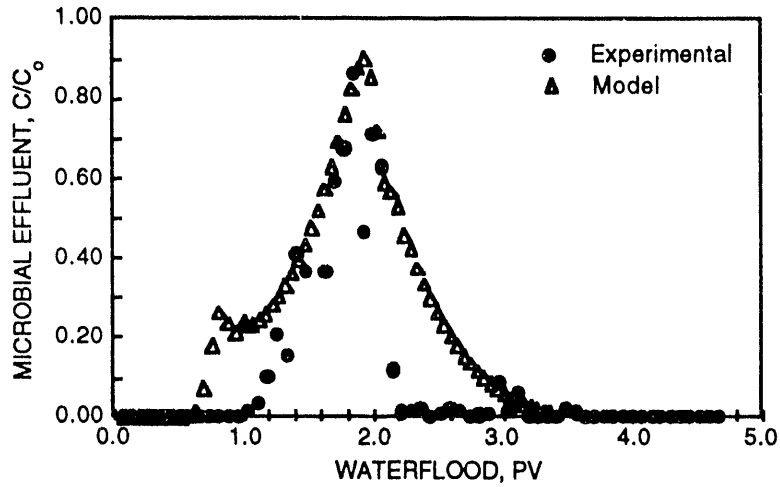

FIGURE 8c. – Simulation match of the microbial concentration in coreflood effluent after 1.5 PV injection.

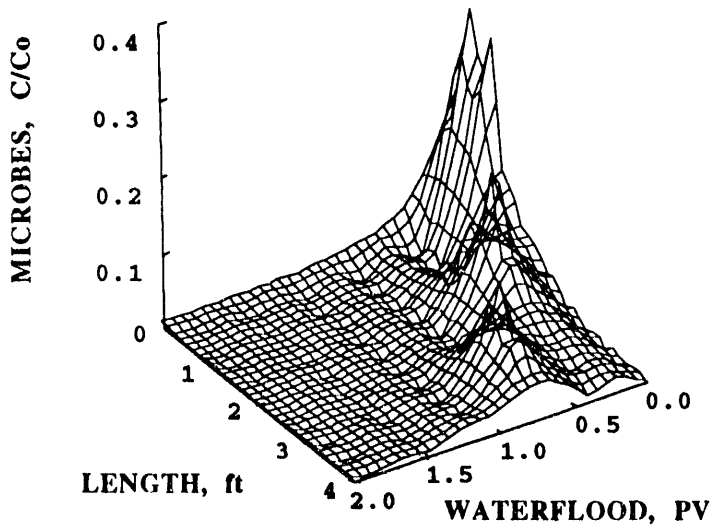

FIGURE 9a. – Results of simulation of the microbial concentration profile through a 4-ft long Berea sandstone core after 0.5 PV waterflood.

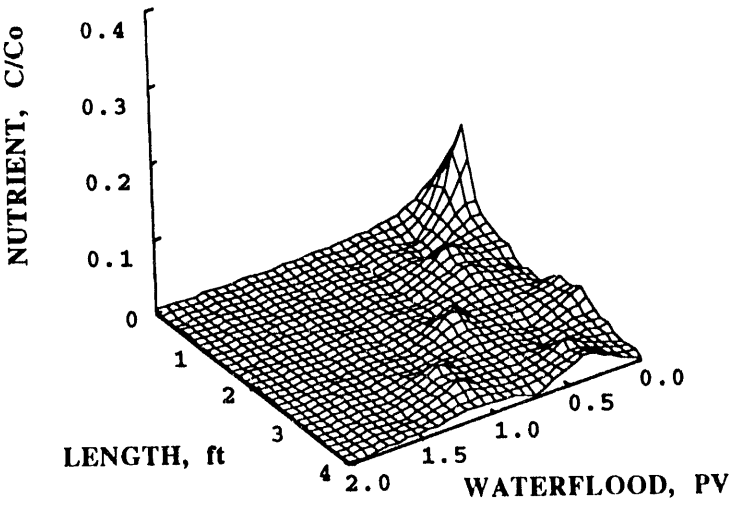

FIGURE 9b. – Results of simulation of the nutrient concentration profile through a 4-ft long Berea sandstone core after 0.5 PV waterflood.

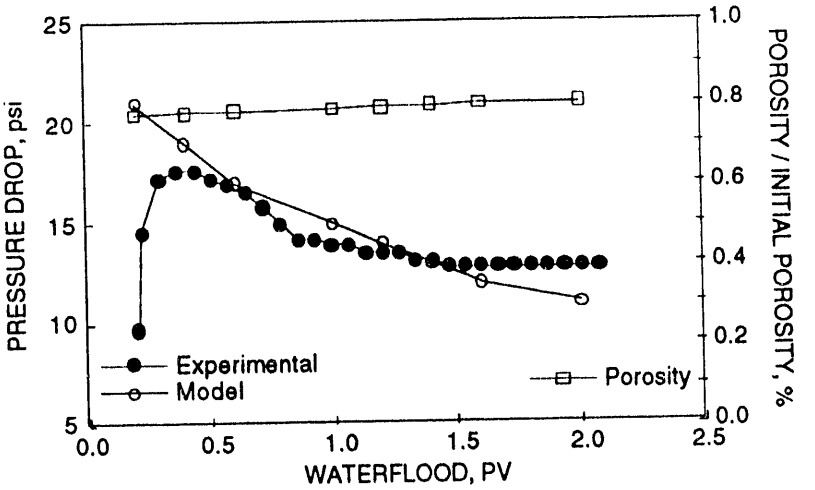

FIGURE 10. – Simulation match of pressure drop and porosity change in a microbial coreflood.

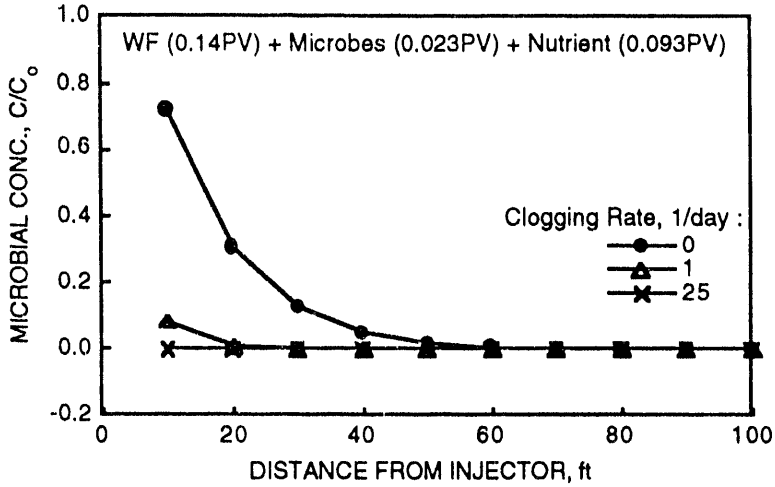

FIGURE 11. – Microbial profiles for reservoirs with various clogging rate constants.

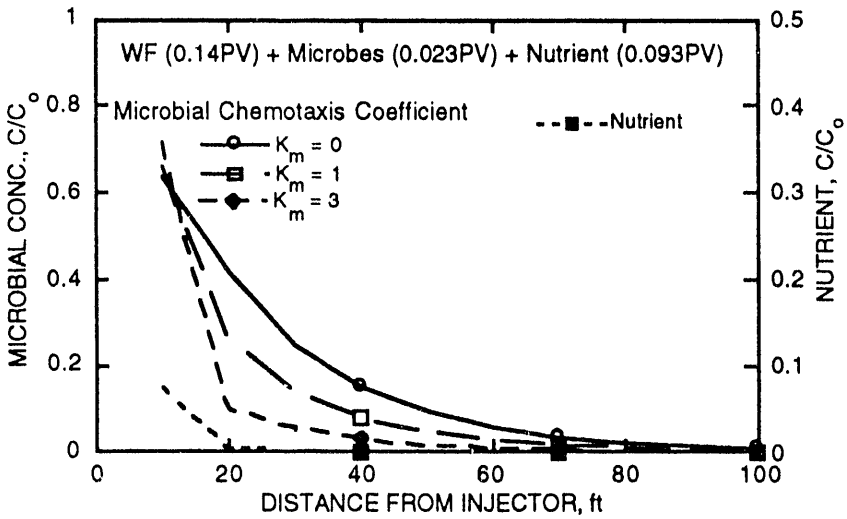

FIGURE 12. – Effect of chemotaxis coefficient k_m on microbial concentration profile.

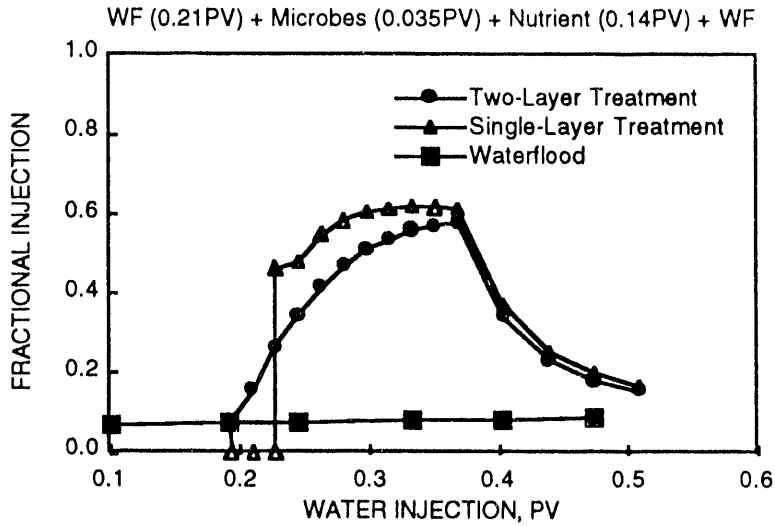

FIGURE 13. – Fractional injection into low permeability layer.

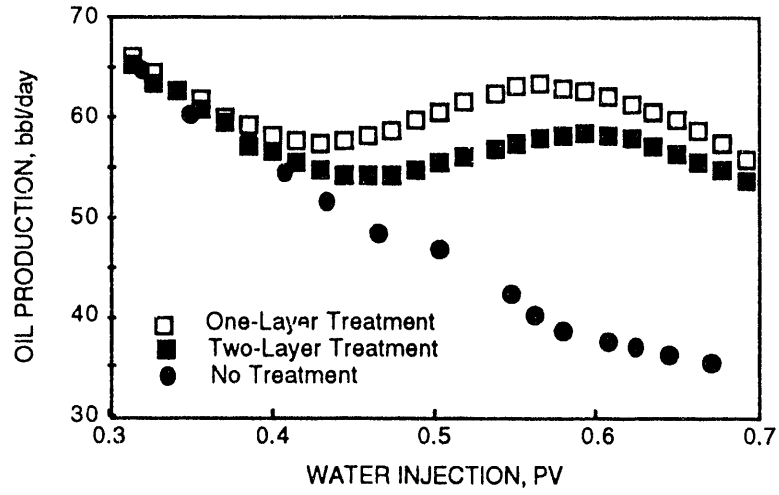

FIGURE 14. – Injection profile modification using microbial treatment.

*U.S.GPO:1992-761-027/60059

DATE
FILMED
02/02/93